UCSF
UC San Francisco Previously Published Works

Title

Antimalarial Benzoxaboroles Target Plasmodium falciparum Leucyl-tRNA Synthetase

Permalink

https://escholarship.org/uc/item/64428066

Journal

Antimicrobial Agents and Chemotherapy, 60(8)

ISSN

0066-4804

Authors

Sonoiki, Ebere
Palencia, Andres
Guo, Denghui
et al.

Publication Date

2016-08-01

DOI

10.1128/aac.00820-16

Peer reviewed

Antimalarial Benzoxaboroles Target *Plasmodium falciparum* Leucyl-tRNA Synthetase

Ebere Sonoiki,[a,b] Andres Palencia,[c] Denghui Guo,[a] Vida Ahyong,[d] Chen Dong,[e] Xianfeng Li,[e] Vincent S. Hernandez,[e] Yong-Kang Zhang,[e] Wai Choi,[e] Jiri Gut,[a] Jennifer Legac,[a] Roland Cooper,[f] M. R. K. Alley,[e] Yvonne R. Freund,[e] Joseph DeRisi,[d] Stephen Cusack,[c] Philip J. Rosenthal[a]

Department of Medicine, University of California, San Francisco, California, USA[a]; Division of Infectious Diseases and Immunology, School of Public Health, University of California, Berkeley, California, USA[b]; European Molecular Biology Laboratory, Grenoble Outstation and Université Joseph Fourier, Centre National de la Recherche Scientifique and EMBL Unit of Virus Host-Cell Interactions, Grenoble, France[c]; Howard Hughes Medical Institute and the Department of Biochemistry and Biophysics, University of California, San Francisco, California, USA[d]; Anacor Pharmaceuticals, Inc., Palo Alto, California, USA[e]; Department of Natural Sciences and Mathematics, Dominican University of California, San Rafael, California, USA[f]

There is a need for new antimalarials, ideally with novel mechanisms of action. Benzoxaboroles have been shown to be active against bacteria, fungi, and trypanosomes. Therefore, we investigated the antimalarial activity and mechanism of action of 3-aminomethyl benzoxaboroles against *Plasmodium falciparum*. Two 3-aminomethyl compounds, AN6426 and AN8432, demonstrated good potency against cultured multidrug-resistant (W2 strain) *P. falciparum* (50% inhibitory concentration [IC_{50}] of 310 nM and 490 nM, respectively) and efficacy against murine *Plasmodium berghei* infection when administered orally once daily for 4 days (90% effective dose [ED_{90}], 7.4 and 16.2 mg/kg of body weight, respectively). To characterize mechanisms of action, we selected parasites with decreased drug sensitivity by culturing with stepwise increases in concentration of AN6426. Resistant clones were characterized by whole-genome sequencing. Three generations of resistant parasites had polymorphisms in the predicted editing domain of the gene encoding a *P. falciparum* leucyl-tRNA synthetase (LeuRS; PF3D7_0622800) and in another gene (PF3D7_1218100), which encodes a protein of unknown function. Solution of the structure of the *P. falciparum* LeuRS editing domain suggested key roles for mutated residues in LeuRS editing. Short incubations with AN6426 and AN8432, unlike artemisinin, caused dose-dependent inhibition of [^{14}C]leucine incorporation by cultured wild-type, but not resistant, parasites. The growth of resistant, but not wild-type, parasites was impaired in the presence of the unnatural amino acid norvaline, consistent with a loss of LeuRS editing activity in resistant parasites. In summary, the benzoxaboroles AN6426 and AN8432 offer effective antimalarial activity and act, at least in part, against a novel target, the editing domain of *P. falciparum* LeuRS.

There is an urgent need for new antimalarials. As older regimens are limited by resistance in *Plasmodium falciparum*, the most virulent human malaria parasite, artemisinin-based combination therapy regimens have been adopted as standard treatment for uncomplicated falciparum malaria (1). However, resistance to artemisinins is growing in Southeast Asia (2), and resistance has been seen to most artemisinin partner drugs (3). Drug resistance seriously jeopardizes efforts to control and eliminate malaria, and new agents, ideally with novel mechanisms of action, are needed.

Benzoxaboroles are boron-containing compounds that have demonstrated potent activity against a number of infectious pathogens, including bacteria (4, 5), fungi (6), and trypanosomes (7). The highly electrophilic nature of the boron component of these compounds leads to interaction with a variety of protein targets via reversible covalent bonds (8, 9), with identified targets including leucyl-tRNA synthetase (LeuRS) (5, 6) and β-lactamase (10). In particular, the benzoxaboroles tavaborole and AN3018 (6) inhibit fungal LeuRS, and AN3365 and AN3664/ZCL039 inhibit bacterial LeuRS (4, 5).

There is increasing interest in the exploration of aminoacyl-tRNA synthetases as antimicrobial targets in both prokaryotic and eukaryotic pathogens (11, 12). These enzymes catalyze the attachment (charging) of amino acids to their cognate tRNAs. For example, mupirocin inhibits bacterial IleRS and is used topically to control *Staphylococcus aureus* colonization (13). Class I aminoacyl-tRNA synthetases, including LeuRS, contain a *cis* editing domain that is distinct from the enzyme active site and that recog-

nizes noncognate amino acids and hydrolyzes misacylated tRNAs (14). The LeuRS editing domain is the target of the benzoxaborole LeuRS inhibitors noted above. In *P. falciparum*, aminoacyl-tRNA synthetase inhibitors and their targets include borrelidin (ThrRS) (15, 16), mupirocin (IleRS) (17), 4-thiaisoleucine (IleRS) (18), cladosporin (LysRS) (19), lysyl-adenylate analogues (LysRS) (20), and halofuginone (ProRS) (21). The *P. falciparum* cytosolic LeuRS, but not an apicoplast-directed LeuRS, contains a typical editing domain (22).

In a search for new antimalarial compounds, we screened a benzoxaborole library rich in LeuRS inhibitors for potency against cultured *P. falciparum*. The two most active compounds, AN6426 and AN8432, were selected for further studies. The compounds

TABLE 1 *In vitro* and *in vivo* antimalarial activities of AN6426 and AN8432[a]

	Cultured parasite IC$_{50}$ (μM)				Mammalian cell CC$_{50}$ (μM)		Murine malaria ED$_{90}$ (mg/kg) (*P. berghei*)
	Laboratory strain						
Compound	3D7	W2	Dd2	Ugandan isolates	HepG2	Jurkat	
AN6426	0.19 ± 0.05	0.31 ± 0.18	0.42 ± 0.15	0.35 ± 0.13	78 ± 3	>100	7.4
AN8432	0.28 ± 0.01	0.49 ± 0.29	0.49 ± 0.18	ND	106 ± 38	>25	16.2

[a] IC$_{50}$ results (± standard deviations) are means from at least 3 experiments, each with duplicate readings. CC$_{50}$ (50% cytotoxic concentration) results for Jurkat and HepG2 cells are means from 2 experiments, each with at least 2 replicates. The value for field isolates is the mean readings from 7 independent isolates collected in Tororo, Uganda, in 2013 and performed as described previously (40). *In vivo* ED$_{90}$ values are based on comparisons of parasitemias between treated and control animals on the fourth day after inoculation of parasites and initiation of treatment. ND, not determined.

demonstrated effective activity against multiple *P. falciparum* strains and in a murine malaria model. Genetic and biochemical evidence is consistent with activity of these compounds against *P. falciparum* LeuRS.

MATERIALS AND METHODS

Synthesis of benzoxaboroles. Experimental procedures and analytical data for compounds 1, 2, 5, 6, 9, and 10 (Table 1) were described previously (23). Their analogs, 3, 4, 7, and 8, were prepared by following similar synthetic routes and procedures. The compounds were analyzed by ^{1}H nuclear magnetic resonance (NMR), liquid chromatography-mass spectrometry (LC-MS), and high-performance liquid chromatography (HPLC) for structural characterization and purity. ^{1}H NMR spectra were recorded on a Varian or Bruker spectrometer (300 or 400 MHz). LC-MS data were obtained using an Agilent LC-MS 1200 with a 6110 MS detector equipped with an electrospray ion source operated in a positive or negative mode. HPLC analysis was performed on a Shimadzu HPLC system or a Waters 600 controller system. The columns used were a Venusil XBP-C$_{18}$ (50 by 4.6 mm inner diameter [ID]), Shimpack VP-ODS (150 by 4.6 mm ID), or UPLC BEH C$_{18}$ (50 by 2.1 mm ID). Resulting analytical data were consistent with corresponding structures, and HPLC purity was ≥95% at 214, 220, or 254 nm (see the supplemental material).

Culture of malaria parasites. Erythrocytic *P. falciparum* was cultured using standard methods at 2% hematocrit in RPMI 1640 (Invitrogen) medium supplemented with 0.5% AlbuMAX II (GIBCO Life Technologies), 2 mM L-glutamine, 100 mM hypoxanthine, 5 μg/ml gentamicin, 28 mM NaHCO$_3$, and 25 mM HEPES at 37°C in an atmosphere of 5% O$_2$, 5% CO$_2$, and 90% N$_2$. *P. falciparum* strains were from the Malaria Research and Reference Reagent Resource Center (https://www.beiresources.org/ProgramInformation.aspx).

Activity of benzoxaboroles against cultured *P. falciparum*. Parasites were synchronized by treatment with 5% D-sorbitol and cultured in duplicate 96-well culture plates (200 μl per well) with serially diluted benzoxaboroles or the antimalarials chloroquine, lumefantrine, mefloquine, piperaquine, artemisinin, and dihydroartemisinin (from Sigma-Aldrich, except piperaquine, which was from Jinan Jiaquan International Trade Co.), at concentrations of 0.056 to 1,000 nM, with ≤0.2% dimethyl sulfoxide (DMSO). After 48 h, cultures were fixed with 2% formaldehyde for 24 h at 37°C or 48 h at room temperature, cells were stained with 4 nM YOYO-1 dye (Molecular Probes), and counts of treated and control cultures were determined using fluorescence-activated cell sorting (FACS). Fifty percent inhibitory concentrations (IC$_{50}$s) were calculated by nonlinear regression using GraphPad Prism software. Activity against isolates from Ugandan children with uncomplicated falciparum malaria was determined using an enzyme-linked immunosorbent assay (ELISA) directed against *P. falciparum* histidine-rich protein-2, as previously described (24).

Cytotoxicity assays. Human Jurkat (T cell lymphoma) and HepG2 (hepatocarcinoma) cells were from the American Type Culture Collection. Jurkat cells were seeded in 96-well plates at 2 × 10^4 cells per well in 100 μl RPMI 1640 medium with 10% fetal bovine serum and 2 mM

L-glutamine, with 10-fold serial dilutions (0.1 nM to 100 μM) of oxaboroles and a final concentration of 0.25% DMSO. Plates were incubated at 37°C in 5% CO$_2$ for 72 h, 20 μl [3-(4,5-dimethylthiazol-2-yl)-5-(3-carboxymethoxyphenyl)-2-(4-sulfophenyl)-2H-tetrazolium] was added, and after 4 additional h, absorbance was determined at 490 and 690 nm. IC$_{50}$s were calculated by nonlinear regression analysis with the four-parameter logistic equation using GraphPad Prism software. HepG2 cells were seeded in 96-well plates at 3,000 cells per well in Dulbecco's modified Eagle's medium with 10% fetal bovine serum, 2 mM L-glutamine, and 50 U/ml penicillin-streptomycin. Serial half-log dilutions of oxaboroles in DMSO, at a final concentration of 0.5% DMSO, were added, and cells were grown for 7 days at 37°C in 5% CO$_2$ with replacement of medium and compounds on the fourth day. After 7 days, medium was removed, cells were blotted dry, 50 μl of 1× Janus green stain (Mitosciences, Eugene, OR) was added per well, and the assay was developed according to the manufacturer's protocol (in-cell ELISA kit; catalog number MS643). Absorbance at 595 nm was measured and IC$_{50}$s were calculated as described for Jurkat cells.

Activity of benzoxaboroles against murine malaria. Swiss Webster mice were infected intraperitoneally with 6 × 10^6 *P. berghei*-infected erythrocytes collected from a previously infected mouse and then treated, beginning 1 h after inoculation, with benzoxaboroles (in 55% polyethylene glycol [PEG] 300, 25% propylene glycol, 20% water) or chloroquine (in water) by daily oral gavage for 4 days. Negative controls were treated with vehicle only. Infections were monitored by daily microscopic evaluation of Giemsa-stained blood smears. ED$_{90}$ values, based on comparisons of parasitemias between treated and control animals on the fourth day after initiation of treatment, were calculated using GraphPad Prism software. Mice were euthanized when parasitemias exceeded 50%.

Stage specificity assay. Using a previously described protocol (25), synchronous W2 strain *P. falciparum* organisms were cultured in triplicate wells in 96-well culture plates with 2 μM AN6426 or 1.3 μM chloroquine for 8-h intervals, beginning at the ring stage. At the end of each interval, the cultures were washed 3 times and resuspended in culture media without drug. After 48 h, when control parasites were at the ring stage, the cultures were fixed with 2% formaldehyde, stained, and counted with FACS as described above.

Selection of parasites with decreased sensitivity to AN6426. Triplicate 10-ml cultures of Dd2 strain *P. falciparum*, each containing a clonal population of 6 × 10^7 asynchronous parasites, were incubated with stepwise increasing concentrations of AN6426, beginning with 0.4 μM. Medium was changed and fresh AN6426 added daily. Once treated parasites grew at rates comparable to those of untreated controls, parasite aliquots were cloned by limiting dilution, drug sensitivity (IC$_{50}$s) was assessed as described above, aliquots were stored, the concentration of AN6426 was increased, and the selection process was repeated. To assess the ease of resistance selection, 3 cultures each of 10^6, 10^7, and 10^8 Dd2 strain parasites were incubated with 1.5 μM AN6426, and cultures were monitored for 67 days or until parasites regrew.

Whole-genome sequencing. To prepare genomic DNA, synchronized *P. falciparum*-infected erythrocytes (100 ml, 2% hematocrit, 10% para-

sitemia) were treated with 0.15% saponin for 5 min on ice to lyse erythrocytes, followed by 3 washes in phosphate-buffered saline (PBS). Parasite pellets were lysed in 150 mM NaCl, 10 mM EDTA, 50 mM Tris-HCl, pH 7.5, 0.1% Sarkosyl (Sigma-Aldrich), and 200 mg/ml proteinase K (Qiagen) overnight at 37°C. The samples were then subjected to extraction with phenol-chloroform–isoamyl alcohol (25:24:1), pH 7.9 (Ambion), treatment with 0.05 mg/ml RNase A (1 h 37°C), two additional phenol-chloroform extractions, one chloroform extraction, and then ethanol precipitation. All extractions used light phase lock tubes (5 Prime).

Genomic DNA libraries were prepared from 100 ng DNA using the Nextera DNA sample preparation kit (Illumina) according to the manufacturer's instructions, except with 6 cycles and the bridge amplification step at 65°C for 6 min (26). Each library was barcoded with unique sets of two indices from the Nextera index kit (Illumina) to allow multiple samples to be run on one flow cell. Fragments of 360 to 560 bp next were extracted and collected using Lab Chip XT (Caliper Life Sciences) according to the manufacturer's instructions. The fragments were amplified by limited-cycle PCR using Kapa HiFi DNA polymerase (Kapa Biosystems) with deoxynucleoside triphosphates (dNTPs) with an 80% AT coding bias (6 cycles of 95°C for 10 s, 58°C for 30 s, 65°C for 6 min). The primers for both PCR steps were AATGATACGGCGACCACCGA and CAAGCAGA AGACGGCATACG (26). Libraries were pooled at concentrations of 2 nM per library, as determined with a DNA Bioanalyzer (Agilent). Final library quantification and qualification, as detailed previously (26), were completed, followed by sequencing at the UCSF Center for Advanced Technology on a HiSeq 2000 system (Illumina). Sequence data for each library were aligned to the 3D7 reference genome using Bowtie (27), discarding reads with >1 nucleotide mismatch and multiple alignments across the genome. For the identification of single-nucleotide polymorphisms (SNPs), reads were matched to those from the parental strain, and the top 200 SNPs per chromosome, ranked according to frequency of conflicting nucleotides per position in the genome, were chosen and filtered based on standard parameters (26). SNPs were considered legitimate if the number of reads covering the position was >10 and the frequency was at least 80%. Searches for novel SNPs included only nonsynonymous SNPs in exons, excluding hypervariable genes (*pfemp1*, *rifin*, and *stevor*). Copy number variation was analyzed using the UCSC Genome Browser (28).

Dideoxy sequencing. Genomic DNA was extracted using the QIAamp DNA minikit (Qiagen) according to the manufacturer's instructions. PF3D7_0622800 was amplified in 4 fragments using the Phusion Hot Start II high-fidelity DNA polymerase kit (Thermo Scientific) with 80% AT dNTPs and primers described in Table S3 in the supplemental material (95°C for 3 min; 30 cycles of 95°C for 10 s, 52°C for 30 s, 65°C for 1 min; 68°C for 10 min). The amplified fragments were cleaned using ExoSAP-IT (Affymetrix), mixed with sequencing primers (see Table S3), and sequenced at the UCSF Genome Core Facility. For PF3D7_1218100, the same approach was followed, but only one 800-bp fragment, including the M416T SNP, was amplified and sequenced.

Production of *P. falciparum* and *P. knowlesi* LeuRS editing domains. DNA fragments encoding LeuRS editing domains of *P. falciparum* (*Pf*LeuRS; residues 272 to 687) and *P. knowlesi* (*Pk*LeuRS; residues 266 to 600) were cloned into the NcoI-XhoI sites of pETM-11 (EMBL). Flexible loops of *Pf*LeuRS (residues 328 to 361 and 475 to 519, corresponding to insertions 1 and 3, respectively) and *Pk*LeuRS (residues 400 to 432) were deleted for crystallization. A glycine was introduced at position 475 of *Pf*LeuRS. Cysteine 273 of *Pf*LeuRS was mutated to serine to prevent formation of intermolecular disulfide bridges. Proteins were expressed in BL21-Codon+RIL *Escherichia coli* at 18°C. The cells were lysed by sonication in 40 to 60 ml of lysis buffer (20 mM Tris-HCl, pH 8.0, 100 mM NaCl, 5 mM β-mercaptoethanol, 10 mM imidazole, and one tablet of cOmplete protease inhibitor [Roche]). The soluble fraction was loaded onto a nickel-nitrilotriacetic column (Ni-NTA; Qiagen) and washed with 50 ml lysis buffer, 50 ml lysis buffer plus 1 M NaCl, and then 50 ml lysis buffer. Proteins were eluted with 15 ml lysis buffer plus 400 mM imidazole. The His tag of recombinant proteins was removed with tobacco

etch virus protease. Pure protein fractions were dialyzed in lysis buffer without imidazole and concentrated to 10 to 15 mg ml^{-1}.

Crystallization of *P. falciparum* and *P. knowlesi* LeuRS editing domains. Crystallization was carried out at 20°C by the hanging-drop vapor diffusion method. *Pf*LeuRS D3 crystallized in two different space groups. Monoclinic crystals of *Pf*LeuRS D3 were obtained by mixing 1 μl 10 mg/ml protein with 1 μl reservoir solution containing 0.2 M sodium nitrate, pH 6.8, 20% (wt/vol) PEG 3350, and 12% glycerol. Triclinic crystals of *Pf*LeuRS D3 were obtained by mixing 1 μl 10 mg/ml protein with 1 μl reservoir solution containing 0.1 M HEPES, pH 7.5, 10% isopropanol, 20% (wt/vol) PEG 4000, and 5% glycerol. Crystals of *Pf*LeuRS D13 were obtained by mixing 1 μl of 10 mg/ml protein with 1 μl reservoir solution containing 0.1 M HEPES, pH 7.5, 20% (wt/vol) PEG 10000, and 8% ethylene glycol. Crystals of *Pk*LeuRS were obtained by mixing 1 μl of protein at 12 mg ml^{-1} with 1 μl reservoir solution containing 0.05 M sodium cacodylate, pH 6.5, 0.2 M potassium chloride, 0.1 M magnesium acetate, 10% (wt/vol) PEG 8000, and 25% ethylene glycol.

Structure determination and refinement. All data collection and refinement statistics are shown in Table S2 in the supplemental material. Diffraction data sets were collected at the European Synchrotron Radiation Facility and integrated and scaled with the XDS suite (29) or with the HKL2000 program package (30). Further data analysis was performed with the CCP4 suite (31). The structure of *Pk*LeuRS D3 was initially solved by molecular replacement with PHASER (32) using the structure of the *Cryptosporidium muris* LeuRS (*Cm*LeuRS) editing domain (PDB entry 5FOM; A. Palencia, R. Liu, M. Lukarska, J. Gut, A. Bougdour, B. Touquet, E. Wang, X. Li, M. R. K. Alley, Y. R. Freund, P. J. Rosenthal, M. Hakimi, and S. Cusack, unpublished data) as a model. All models were improved by manual adjustments with COOT (33) and refined using REFMAC5 (34). Structure quality was analyzed with the PDBe validation server (http://wwpdb-validation.wwpdb.org/validservice/), which showed all residues for the different models in allowed regions of the Ramachandran plot. Figures were drawn with PYMOL (http://www.pymol.org/). Docking of AN6426-Ade76 into the editing site of plasmodial LeuRS was done by structural alignment of the *Pf*LeuRS structure to the complex of *Cm*LeuRS-AN6426-AMP (PDB entry 5FOM). The root-mean-square deviation calculated over backbone atoms of *Cm*LeuRS and *Pf*LeuRS was 1.27 Å.

Protein synthesis assay. Synchronous Dd2 strain trophozoites at 10 to 15% parasitemia were washed 3 times with leucine-free culture medium and resuspended at 5% hematocrit in the same medium. Triplicate 100-μl cultures were incubated with 0×, 1×, 10×, or 100× the IC$_{50}$ of test compounds for 15 min at 37°C, 0.5 μCi of [^{14}C]leucine (324 mCi/mmol; PerkinElmer) was added, cultures were incubated for 2 h at 37°C, erythrocytes were lysed with 0.15% saponin as described above, pellets were resuspended in 100 μl 0.02% sodium deoxycholate (Sigma-Aldrich) to lyse the parasites, and 100 μl ice-cold 10% (wt/vol) trichloroacetic acid (TCA) was added to precipitate proteins. Precipitates were transferred to 0.45-μm nitrocellulose membrane filter plates (Millipore Multiscreen HTS, MSHAN4B50), washed 4 times with 400 μl ice-cold 5% TCA, and air dried. [^{14}C]leucine incorporation was determined by adding 60 μl OptiPhase Supermix scintillation cocktail (PerkinElmer) and counting in a Wallac MicroBeta Trilux 1450 liquid scintillation counter.

Norvaline sensitivity assay. Synchronized Dd2 strain parasites were cultured at 1% parasitemia, beginning at the ring stage, in either leucine-free or complete culture media with various concentrations of L-norvaline (Sigma-Aldrich) for 48 h, and the parasites were then fixed, stained, and counted as described above.

Protein structure accession numbers. Atomic coordinates and structure factors have been deposited in the Protein Data Bank under the following accession codes: 5FO4 for the *Pf*LeuRS D3 structure in the P1 space group, 5FOC for *Pf*LeuRS D3 in the P2$_1$ space group, 5FOD for the *Pf*LeuRS D13 structure, and 5FOF for the *Pk*LeuRS structure.
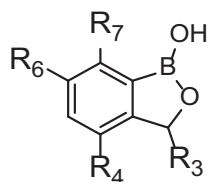
Entry	R_3	R_4	R_6	R_7	$cLogD_{7.4}$	IC50 (µM)
1	NH_2CH_2	Ph	H	EtO	1.8	2.7
2	NH_2CH_2	Cl	H	EtO	0.68	0.71
3	NH_2CH_2	Cl	H	$PhCH_2O$	2.1	0.84
4	NH_2CH_2	Cl	Cl	EtO	1.2	3.3
5	$BocNHCH_2$	Cl	H	EtO	2.8	>10
6 (AN6426)	(S)-NH_2CH_2	Cl	H	EtO	0.68	0.31
7	(S)-NH_2CH_2	Cl	H	MeO	0.34	0.86
8	(S)-NH_2CH_2	Cl	H	c-PrO	0.73	2.8
9	(S)-NH_2CH_2	F	H	EtO	0.29	2.2
10 (AN8432)	(S)-NH_2CH_2	Br	H	EtO	0.95	0.49
Artemisinin						0.006
Chloroquine						0.10

FIG 1 *In vitro* activity of benzoxaboroles against cultured *P. falciparum*. IC$_{50}$s against the W2 strain of *P. falciparum* were determined from two independent experiments, each performed in duplicate. cLogD$_{7.4}$ (calculated [log] distribution coefficient at pH 7.4) was calculated using ChemAxon software under the condition of pH 7.4. Boc, *tert*-butoxycarbonyl.

RESULTS

Structure-activity relationships for 3-aminomethyl benzoxaboroles active against *P. falciparum*. A benzoxaborole library was screened against cultured multidrug-resistant W2 strain *P. falciparum*. Multiple 3-aminomethyl benzoxaboroles were active, and IC$_{50}$s were determined for the closely related compounds 1 to 10 (Fig. 1). Compound 1, with a phenyl group at R$_4$, had moderate activity; replacement with a chloro atom in compound 2 led to submicromolar activity. Larger and more lipophilic groups at R$_7$, such as a 7-benzyloxy group in compound 3, had minimal effect on antimalarial activity. A free basic amino group at R$_3$ was required for activity, as a Boc-blocked amino group abrogated activity in compound 5. Replacement of the R$_7$ ethoxy group (compound 6; AN6426) with other alkoxy groups, such as methoxy in 7 and cyclopropyloxy in 8, led to decreased activity. Replacement of the R$_4$ Cl with F in compound 9 reduced activity; replacement of this Cl with Br (10; AN8432) had minimal impact on activity. From this analysis, compounds AN6426 and AN8432 emerged as the most active antimalarials, and they were selected for further study.

***In vitro* and *in vivo* antimalarial activity of AN6426 and AN8432.** We characterized activities of AN6426 and AN8432 against multiple strains of *P. falciparum*, including field isolates. Activities were similar against laboratory strains known to be sensitive (3D7) or resistant (W2 and Dd2) to chloroquine and other antimalarials and against fresh isolates collected from malaria patients in Uganda in 2012 (Table 1). Assessment of IC$_{50}$s showed minimal differences after 48- or 96-h incubations; thus, AN6426

and AN8432 lack the delayed death phenotype (with much greater activity after 96 h) seen with tetracyclines and some other antimicrobials. The compounds were tested for cytotoxicity against human Jurkat and HepG2 cells; toxicity was seen only at concentrations at least 50-fold greater than concentrations toxic to cultured parasites.

When administered orally to *P. berghei*-infected mice once daily for 4 days, the compounds demonstrated activity, with day 4 ED$_{90}$ values of 7.4 mg/kg/day for AN6426 and 16.2 mg/kg/day for AN8432. At a dosage of 200 mg/kg/day, the compounds afforded long-term cures in 40 to 60% of infected mice (see Fig. S1 in the supplemental material).

Stage specificity and morphological effects of AN6426. Synchronized W2 strain parasites were incubated with the compound or chloroquine for 8-h intervals across the erythrocytic life cycle. AN6426 was removed at 8-h time points, cultures were maintained until untreated control parasites had reached the ring stage, and the parasitemias of control and treated cultures were compared. For both AN6426 and chloroquine, inhibition of parasite development was seen across the life cycle, but activity was greatest against trophozoites (Fig. 2). AN6426-treated parasites had no obvious morphological abnormalities during the ring and early trophozoite stages, but the parasites treated during these stages were unable to develop into multinucleated schizonts or new ring-stage parasites (Fig. 2).

Selection and analysis of parasites with decreased sensitivity to AN6426. To gain insight into the antimalarial mechanism of action of AN6426, we cultured Dd2 strain *P. falciparum* in step-
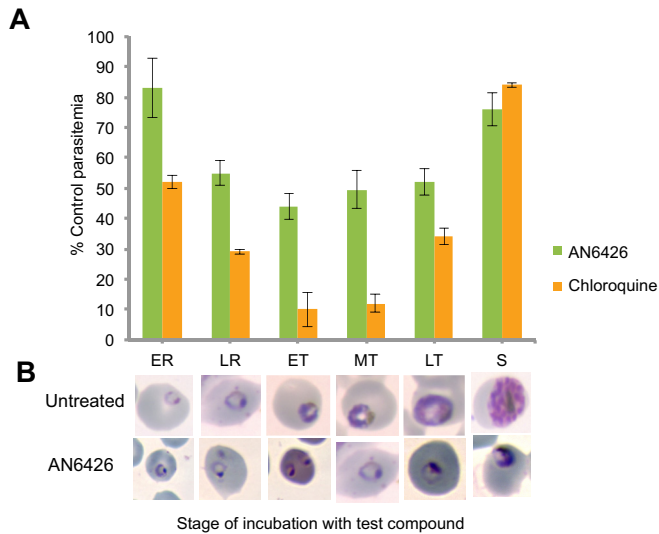
FIG 2 Stage specificity of action of AN6426. (A) Parasitemias were compared between W2 strain *P. falciparum* incubated with 2 μM AN6426, 1.3 μM chloroquine, or 0.1% DMSO for 8-h intervals across the life cycle and then continued in culture until the following ring stage, when parasitemias were counted and compared. Error bars represent standard deviations from 3 independent experiments. (B) Photomicrographs of representative parasites treated with AN6426 and untreated controls are shown. ER and LR, early and late rings; ET, MT, and LT, early, mid-stage, and late trophozoites; S, schizonts.

wise increasing concentrations of the compound, assessed parasite sensitivity after each step, and characterized cloned parasites with decreased sensitivity by whole-genome sequencing. Parasites were incubated with AN6426 at 0.4 μM for 4 weeks (R1), 1 μM for 10 weeks (R2), and then 10 μM for 14 weeks (R3) (Fig. 3). At each step of selection, parasites were initially undetectable on Giemsa-stained smears (for ~3 weeks for R1 and 7 to 8 weeks for R2 and R3) followed by regrowth, suggesting selection of mutations allowing growth under drug pressure. Parasites at each step of AN6426 resistance were similarly resistant to AN8432, indicative of a shared mechanism of resistance. In contrast, selected parasites did not demonstrate decreased sensitivity to the antimalarials

chloroquine, lumefantrine, mefloquine, piperaquine, and dihydroartemisinin (Fig. 3).

Parasites from each step of selection were cloned by limiting dilution, and DNA from multiple clones was analyzed by whole-genome sequencing. Sequencing identified a number of genetic changes between parent and AN6426-resistant parasites, including SNPs and copy number variations. SNPs in only two genes were seen in multiple clones from all selection steps: PF3D7_0622800, which encodes cytoplasmic LeuRS (35), and PF3D7_1218100, which encodes a protein of unknown function classified as a membrane protein based on homology models (36). For the LeuRS gene, 4 different SNPs were identified in the predicted editing domain (14, 37, 38) (Fig. 3). SNPs identified in R2 and R3 parasites (T400I and V568L), but not those identified in R1 parasites (E628G and V630L), map to conserved editing active-site regions of LeuRS from other eukaryotic pathogens (Fig. 4). For PF3D7_1218100, a single SNP (M416T) was present in R1, R2, and R3 parasites (Fig. 3). In addition, 2- to 4-fold amplification of two clusters of genes on chromosome 12 was observed at all levels of resistance; one of these clusters includes PF3D7_1218100 (see Table S1 in the supplemental material). R3 parasites were subsequently cultured without drug pressure for 5 months. These parasites showed partial reversion to drug sensitivity, with ~5-fold decreased sensitivity to AN6426 compared to the wild type, but they retained mutations in both PF3D7_0622800 and PF3D7_1218100.

To assess ease of selection of resistance to AN6426, we cultured different numbers of Dd2 strain *P. falciparum* with 1.5 μM AN6426. In 3 cultures with inocula of 10^8 parasites, parasites regrew after 16, 23, and 23 days. With 3 cultures each of 10^7 or 10^6 parasites, no growth was seen over 67 days of observation. For parasites incubated with 5 nM atovaquone, all 6 cultures with inocula of 10^8 parasites regrew over 24 to 50 days, 2 of 6 cultures with inocula of 10^7 parasites regrew after 45 days, and 1 of 6 cultures with inocula of 10^6 parasites regrew after 45 days.

Structure of the LeuRS editing domain of *P. falciparum* and *P. knowlesi*. To better understand AN6426-LeuRS interactions, we obtained crystal structures of the editing domain from two plasmodial species. Based on the crystal structure of the LeuRS editing domain of the related apicomplexan parasite *Cryptospo-*
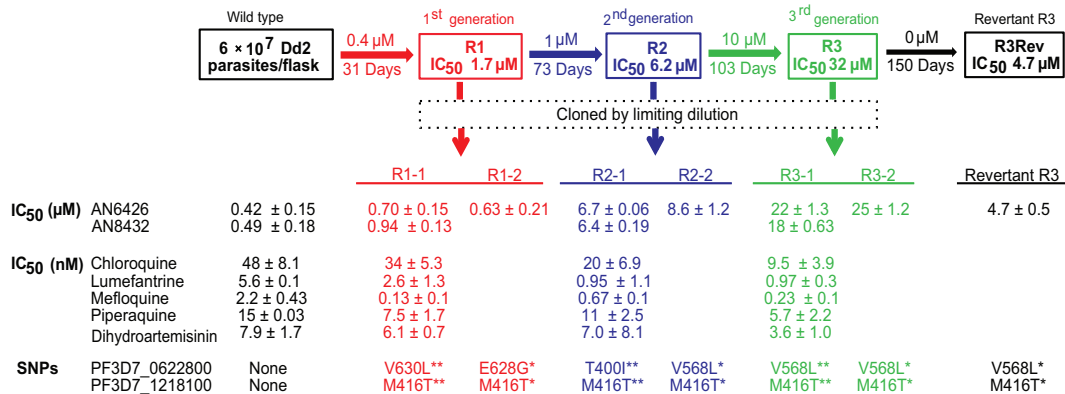

FIG 3 Selection and analysis of AN6426-resistant parasites. The selection schematic is shown at the top, including concentration of AN6426 and duration of incubation for each step. IC_{50}s for the indicated compounds are shown after each selection; values include standard deviations from at least 3 independent experiments, each with 2 replicates. SNPs identified in these parasites by whole-genome and dideoxy sequencing (**) or by dideoxy sequencing alone (*), based on comparison with the 3D7 reference strain, are shown.
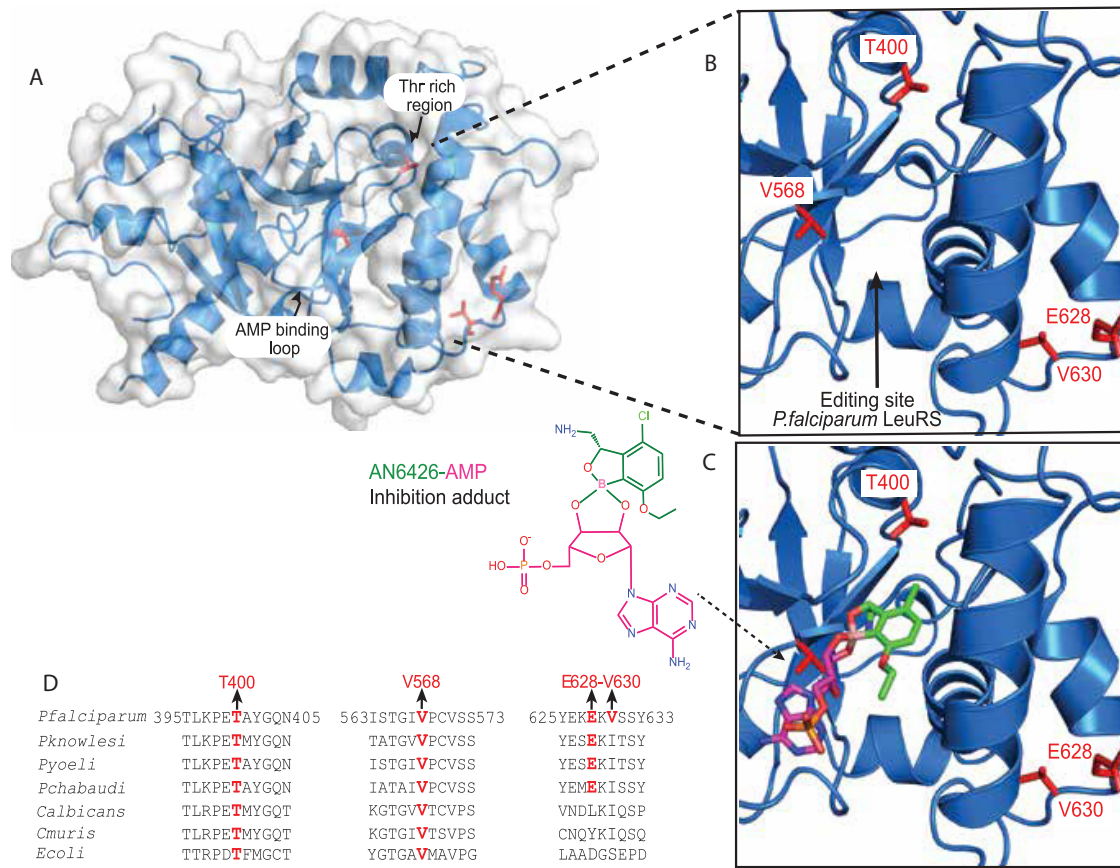
FIG 4 Structure of *P. falciparum* LeuRS editing domain and mapping of resistant mutants. (A) *P. falciparum* LeuRS editing domain surface model (white) and cartoon representation (blue) with resistance mutant residues shown as red sticks. (B) Zoomed view of the *Pf*LeuRS editing site. (C) Docking of AN6426-AMP adduct into the editing site of *Pf*LeuRS. The adduct was placed by overlapping *Pf*LeuRS with the complex of *C. muris* LeuRS with AN6426-AMP (PDB entry 5FOM). Root mean square deviation over backbone atoms was 1.3 Å. (D) Sequence alignment of LeuRSs of plasmodia, other eukaryotic pathogens, and *E. coli*. Residues that are changed in *P. falciparum* AN6426-resistant mutants are highlighted in red.

ridium muris (Palencia et al., unpublished), we designed several constructs of the LeuRS editing domains of *P. falciparum* (residues 272 to 687) and of *P. knowlesi* (residues 266 to 600), a monkey species that causes human infections in Southeast Asia. One or more of three apicomplexan-specific and presumably flexible insertions were deleted with the aim of promoting crystallization. Crystals were obtained for two *P. falciparum* LeuRS constructs, one with deletion of insertion 3 (residues 475 to 520; *Pf*LeuRS D3) and another with deletion of insertion 1 as well (residues 328 to 360; *Pf*LeuRS D13). These crystals diffracted to 1.5 and 1.7 Å, respectively (see Table S2 and Fig. S2 and S3 in the supplemental material). In addition, we obtained crystals of *Pf*LeuRS D3 in a second space group (P1), which diffracted to 1.85 Å. A construct with deletion of insertion 3 in the *P. knowlesi* LeuRS editing domain (*Pk*LeuRS D3) gave crystals diffracting to 2.4 Å (see Table S2). All structures showed the canonical editing domain fold of eukaryotic LeuRS (39) but with unique partially ordered insertions similar to those observed in the LeuRS editing domain of *C. muris* (Palencia et al., unpublished). The role of these insertions, which are distant from the editing active site, is unknown.

The two mutations identified in R2 and R3 resistant parasites, T400I and V568L, map to the threonine-rich and AMP-binding loops of the *P. falciparum* LeuRS editing domain, respectively.

Both loops are involved in binding and proofreading of noncognate amino acids in bacterial and fungal LeuRS homologs (40) and in binding of benzoxaboroles (6, 7, 23, 39). T400 in the *P. falciparum* LeuRS structure aligns with T252 of *E. coli* LeuRS; this residue is responsible for steric exclusion of cognate leucine from the editing site, thereby preventing hydrolysis of correctly charged Leu-tRNA^{Leu} but allowing hydrolysis of incorrectly incorporated amino acids (41). The replacement of threonine with the more bulky isoleucine would likely impact negatively on the predicted binding of AN6426, which extends into the noncognate amino acid binding site. V568 structurally aligns to V335 of *E. coli* LeuRS, which establishes hydrophobic contacts with the terminal adenosine-ribose of the tRNA and is important for the stabilization of the substrate in the LeuRS editing site (40). The V568L substitution is predicted to destabilize or impede the formation of the inhibition adduct (AN6426-AMP) in the editing site of *P. falciparum* LeuRS due to the larger size of leucine. The LeuRS mutations found in R1 resistant parasites, E628G and V630L, which are associated with low-level resistance, map outside the editing active site (Fig. 4).

AN6426 and AN8432 inhibit protein synthesis. To further consider *P. falciparum* LeuRS as the target for the 3-aminomethyl benzoxaboroles, we characterized the effects of AN6426 and
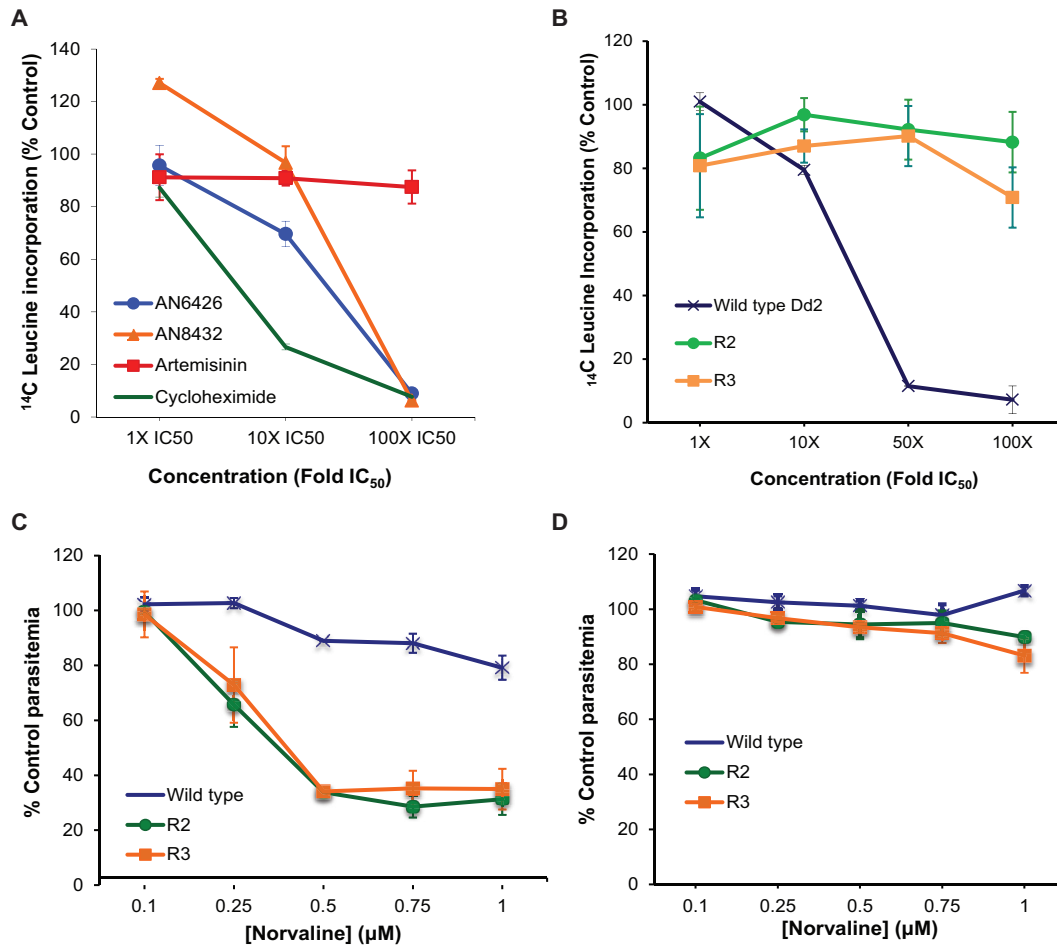
FIG 5 Biochemical support for action of benzoxaboroles against LeuRS. (A) Effects of benzoxaboroles and positive (cycloheximide) and negative (artemisinin) controls on [^{14}C]leucine incorporation by wild-type Dd2 strain *P. falciparum*. (B) Effects of AN6426 on [^{14}C]leucine incorporation by parasites selected for resistance. Concentrations studied were multiples of IC$_{50}$s, determined based on triplicate measures (IC$_{50}$ for AN6426, 420 nM; cycloheximide, 130 nM; artemisinin, 8.7 nM). (C and D) Effects of norvaline on growth of cultured parasites selected for resistance in the absence (C) or presence (D) of exogenous leucine (0.025 g/liter). Error bars represent standard deviations from at least three independent experiments.

AN8432 on uptake of leucine, an indicator of parasite protein synthesis. Treatment of wild-type Dd2 strain parasites with 2-h pulses of AN6426 or AN8432 inhibited incorporation of [^{14}C]leucine, indicative of a block in protein synthesis, as also seen with the protein synthesis inhibitor cycloheximide but not with artemisinin, a rapid-acting antimalarial that does not act against protein synthesis (Fig. 5A). In parasites with high-level resistance to AN6426, the compound did not inhibit [^{14}C]leucine incorporation (Fig. 5B). To specifically assess LeuRS editing, we cultured parasites in leucine-free medium in the presence of norvaline, a noncognate analogue of leucine that is readily charged to tRNA by LeuRS enzymes (40) and then hydrolyzed from tRNA^{Leu} by the editing active site (37). Misincorporation of norvaline into proteins is toxic (6). Norvaline was not toxic to wild-type parasites but markedly inhibited the growth of R2 and R3 parasites (Fig. 4C), an effect that was not seen when cultures contained leucine (Fig. 4D). These results support the hypothesis that AN6426 acts against *P. falciparum* through inhibition of LeuRS editing.

DISCUSSION

We identified two benzoxaboroles, AN6426 and AN8432, with nanomolar *in vitro* activity against *P. falciparum* and efficacy in a

rodent malaria model. To gain insight into mechanisms of action, we selected and characterized parasites with markedly decreased sensitivities to AN6426. Resistant clones consistently showed SNPs predicted to be within the editing domain of LeuRS. Biochemical studies showed that AN6426 and AN8432 inhibited protein synthesis in wild-type, but not AN6426-resistant, parasites, and that resistant parasites were inhibited by exogenous norvaline, consistent with a loss of LeuRS editing. Taken together, our data suggest that a target of the antimalarial benzoxaboroles AN6426 and AN8432 is *P. falciparum* LeuRS.

The mutations seen in parasites selected for resistance to AN6426 were predicted, based on comparison with homologs from other organisms, to be located within the LeuRS editing domain (4–6, 42), and this conclusion was supported by determination of the structure of this domain in *P. falciparum* LeuRS and by our biochemical studies. Brief incubations with AN6426 and AN8432, but not the rapid-acting antimalarial artemisinin, led to dose-dependent inhibition of parasite incorporation of leucine, consistent with a block in protein synthesis. Cycloheximide blocked leucine incorporation at concentrations closer to its antiparasitic IC$_{50}$, presumably because its action against polypeptide elongation (43, 44) is

more rapidly toxic to parasites than inhibition of aminoacylation. In leucine-free media, growth of AN6426-resistant, but not wild-type, parasites was inhibited by norvaline, consistent with a block in LeuRS editing in resistant parasites. Taken together, our genetic and biochemical results suggest that AN6426 and AN8432 act against *P. falciparum* via inhibition of LeuRS.

In contrast to the case for *C. muris*, we did not detect binding of the AN6426-AMP adduct into the isolated *P. falciparum* LeuRS editing domain *in vitro*. Although the *P. falciparum* and *C. muris* editing domain structures are similar (sequence similarity of 38.4%, with root-mean-squared deviation calculated over backbone atoms of 1.3 Å), the *P. falciparum* editing active site contains three idiosyncratic amino acid substitutions (also seen in plasmodial homologs) at usually conserved residues. These substitutions might explain differences in the ease of binding of AN6426 to the editing domain (Fig. 4; also see Fig. S3 in the supplemental material). In *P. falciparum* LeuRS, K397 makes a unique hydrogen bond to Q649 but does not interact with nearby E399. In LeuRS of *C. muris* and many other organisms, these three residues are R397, E649, and E399, and the multivalent arginine forms a salt bridge to both glutamates. Another *P. falciparum*-specific residue, I563, which in other species is a lysine, is predicted to lead to the loss of interaction with the phosphate of the 3′ terminal adenosine (Ade76) of tRNA^{Leu}; this interaction contributes to trapping the tRNA^{Leu} in the editing site of LeuRS. These idiosyncratic differences make it plausible that for *P. falciparum*, unlike other LeuRS enzymes, high-affinity adduct formation occurs only in the context of the full-length LeuRS and tRNA.

Of note, *P. falciparum* encodes two LeuRS enzymes, the nuclear-encoded enzyme that is expressed in the cytoplasm and that we have shown to be the target of AN6426 and a second enzyme that is encoded by the apicoplast genome (PF3D7_0828200; previously annotated PF08_0011) (45). We did not see mutations in the apicoplast LeuRS gene in parasites selected for resistance to AN6426. This result is consistent with the observation that AN6426 targets the LeuRS editing domain and the understanding from informatics analysis that, unlike the cytoplasmic LeuRS, the *P. falciparum* apicoplast LeuRS does not contain a canonical editing domain (46).

Parasites selected for resistance to AN6426 consistently contained an SNP in a second *P. falciparum* gene, PF3D7_1218100, and 2- to 4-fold amplification of a gene cluster that includes this gene. The function of the PF3D7_1218100 product is unknown. The product is predicted to be a 55.7-kDa protein that features two transmembrane domains and an apicoplast signal peptide (36). The gene is transcribed in mature erythrocytic parasites and in sexual stages. Disruption of the *P. berghei* ortholog of PF3D7_1218100 (PBANKA_143370) led to a defect in the development of sporozoites but no apparent effect in erythrocytic parasites (35). Thus, the limited available data concerning this gene product do not explain its role in resistance to AN6426 and AN8432. Further consideration of both LeuRS and the product of PF3D7_1218100 as targets of AN6426 should include reverse genetic experiments to explore the impact of gene alterations on sensitivity to the compound.

Malaria drug discovery is especially challenging. In addition to obvious requirements for a drug to be safe and efficacious, antimalarial drug candidates should meet additional criteria, including rapid clinical response, requirement for no more than 3 days of treatment (and ideally single-dose treatment), oral bioavailabil-

ity, low tendency to select for drug resistance, lack of cross-resistance with existing antimalarials, safety in children and in pregnancy, and low cost of production (47). Our results with AN6426 and AN8432 suggest that the 3-aminomethyloxaborole class warrants further exploration. First, the compounds exerted good activity against *P. falciparum*, although increased potency is a goal in optimization of this class. Second, the compounds were active against murine malaria with once-daily dosing. Third, the safety of other benzoxaboroles has been demonstrated, with extensive *in vitro* and *in vivo* toxicology studies and progression to trials in humans (22, 48, 49). Fourth, AN6426 and related benzoxaboroles are easy to synthesize, requiring a 4- to 6-step scheme starting from inexpensive reagents (50). Lastly, our results suggest that AN6426 has a novel antimalarial mechanism of action, the inhibition of *P. falciparum* LeuRS. Taken together, these results support continued efforts to develop 3-aminomethyl benzoxaboroles as novel antimalarial agents.

REFERENCES

1. White NJ, Pukrittayakamee S, Hien TT, Faiz MA, Mokuolu OA, Dondorp AM. 2014. Malaria. Lancet 383:723–735. http://dx.doi.org/10.1016/S0140-6736(13)60024-0.

2. Ashley EA, Dhorda M, Fairhurst RM, Amaratunga C, Lim P, Suon S, Sreng S, Anderson JM, Mao S, Sam B, Sopha C, Chuor CM, Nguon C, Sovannaroth S, Pukrittayakamee S, Jittamala P, Chotivanich K, Chutasmit K, Suchatsoonthorn C, Runcharoen R, Hien TT, Thuy-Nhien NT, Thanh NV, Phu NH, Htut Y, Han KT, Aye KH, Mokuolu OA, Olaosebikan RR, Folaranmi OO, Mayxay M, Khanthavong M, Hongvanthong B, Newton PN, Onyamboko MA, Fanello CI, Tshefu AK, Mishra N, Valecha N, Phyo AP, Nosten F, Yi P, Tripura R, Borrmann S, Bashraheil M, Peshu J, Faiz MA, Ghose A, Hossain MA, Samad R, Rahman MR, Hasan MM, Islam A, Miotto O, Amato R, Macinnis B, Stalker J, Kwiatkowski DP, Bozdech Z, Jeeyapant A, Cheah PY, Sakulthaew T, Chalk J, Intharabut B, Silamut K, Lee SJ, Vihokhern B, Kunasol C, Imwong M, Tarning J, Taylor WJ, Yeung S, Woodrow CJ, Flegg JA, Das D, Smith J, Venkatesan M, Plowe CV, Stepniewska K, Guerin PJ, Dondorp AM, Day NP, White NJ, Tracking Resistance to Artemisinin Collaboration (TRAC). 2014. Spread of artemisinin resistance in Plasmodium falciparum malaria. N Engl J Med 371:411–423. http://dx.doi.org/10.1056/NEJMoa1314981.

3. Rosenthal PJ. 2013. The interplay between drug resistance and fitness in malaria parasites. Mol Microbiol 89:1025–1038. http://dx.doi.org/10.1111/mmi.12349.

4. Hernandez V, Crepin T, Palencia A, Cusack S, Akama T, Baker SJ, Bu

W, Feng L, Freund YR, Liu L, Meewan M, Mohan M, Mao W, Rock FL, Sexton H, Sheoran A, Zhang Y, Zhang YK, Zhou Y, Nieman JA, Anugula MR, Keramane el M, Savariraj K, Reddy DS, Sharma R, Subedi R, Singh R, O'Leary A, Simon NL, De Marsh PL, Mushtaq S, Warner M, Livermore DM, Alley MR, Plattner JJ. 2013. Discovery of a novel class of boron-based antibacterials with activity against gram-negative bacteria. Antimicrob Agents Chemother 57:1394–1403. http://dx.doi.org/10.1128/AAC.02058-12.

5. Hu QH, Liu RJ, Fang ZP, Zhang J, Ding YY, Tan M, Wang M, Pan W, Zhou HC, Wang ED. 2013. Discovery of a potent benzoxaborole-based anti-pneumococcal agent targeting leucyl-tRNA synthetase. Sci Rep 3:2475.

6. Rock FL, Mao W, Yaremchuk A, Tukalo M, Crepin T, Zhou H, Zhang YK, Hernandez V, Akama T, Baker SJ, Plattner JJ, Shapiro L, Martinis SA, Benkovic SJ, Cusack S, Alley MR. 2007. An antifungal agent inhibits an aminoacyl-tRNA synthetase by trapping tRNA in the editing site. Science 316:1759–1761. http://dx.doi.org/10.1126/science.1142189.

7. Jacobs RT, Nare B, Wring SA, Orr MD, Chen D, Sligar JM, Jenks MX, Noe RA, Bowling TS, Mercer LT, Rewerts C, Gaukel E, Owens J, Parham R, Randolph R, Beaudet B, Bacchi CJ, Yarlett N, Plattner JJ, Freund Y, Ding C, Akama T, Zhang YK, Brun R, Kaiser M, Scandale I, Don R. 2011. SCYX-7158, an orally-active benzoxaborole for the treatment of stage 2 human African trypanosomiasis. PLoS Negl Trop Dis 5:e1151. http://dx.doi.org/10.1371/journal.pntd.0001151.

8. Baker SJ, Ding CZ, Akama T, Zhang YK, Hernandez V, Xia Y. 2009. Therapeutic potential of boron-containing compounds. Future Med Chem 1:1275–1288. http://dx.doi.org/10.4155/fmc.09.71.

9. Baker SJ, Tomsho JW, Benkovic SJ. 2011. Boron-containing inhibitors of synthetases. Chem Soc Rev 40:4279–4285. http://dx.doi.org/10.1039/c0cs00131g.

10. Xia Y, Cao K, Zhou Y, Alley MR, Rock F, Mohan M, Meewan M, Baker SJ, Lux S, Ding CZ, Jia G, Kully M, Plattner JJ. 2011. Synthesis and SAR of novel benzoxaboroles as a new class of beta-lactamase inhibitors. Bioorg Med Chem Lett 21:2533–2536. http://dx.doi.org/10.1016/j.bmcl.2011.02.024.

11. Pham JS, Dawson KL, Jackson KE, Lim EE, Pasaje CF, Turner KE, Ralph SA. 2014. Aminoacyl-tRNA synthetases as drug targets in eukaryotic parasites. Int J Parasitol Drugs Drug Resist 4:1–13. http://dx.doi.org/10.1016/j.ijpddr.2013.10.001.

12. Vondenhoff GH, Van Aerschot A. 2011. Aminoacyl-tRNA synthetase inhibitors as potential antibiotics. Eur J Med Chem 46:5227–5236. http://dx.doi.org/10.1016/j.ejmech.2011.08.049.

13. Gurney R, Thomas CM. 2011. Mupirocin: biosynthesis, special features and applications of an antibiotic from a gram-negative bacterium. Appl Microbiol Biotechnol 90:11–21. http://dx.doi.org/10.1007/s00253-011-3128-3.

14. Ling J, Reynolds N, Ibba M. 2009. Aminoacyl-tRNA synthesis and translational quality control. Annu Rev Microbiol 63:61–78. http://dx.doi.org/10.1146/annurev.micro.091208.073210.

15. Novoa EM, Camacho N, Tor A, Wilkinson B, Moss S, Marin-Garcia P, Azcarate IG, Bautista JM, Mirando AC, Francklyn CS, Varon S, Royo M, Cortes A, Ribas de Pouplana L. 2014. Analogs of natural aminoacyl-tRNA synthetase inhibitors clear malaria in vivo. Proc Natl Acad Sci U S A 111:E5508–E5517. http://dx.doi.org/10.1073/pnas.1405994111.

16. Otoguro K, Ui H, Ishiyama A, Kobayashi M, Togashi H, Takahashi Y, Masuma R, Tanaka H, Tomoda H, Yamada H, Omura S. 2003. In vitro and in vivo antimalarial activities of a non-glycosidic 18-membered macrolide antibiotic, borrelidin, against drug-resistant strains of Plasmodia. J Antibiot (Tokyo) 56:727–729. http://dx.doi.org/10.7164/antibiotics.56.727.

17. Sugawara A, Tanaka T, Hirose T, Ishiyama A, Iwatsuki M, Takahashi Y, Otoguro K, Omura S, Sunazuka T. 2013. Borrelidin analogues with antimalarial activity: design, synthesis and biological evaluation against Plasmodium falciparum parasites. Bioorg Med Chem Lett 23:2302–2305. http://dx.doi.org/10.1016/j.bmcl.2013.02.075.

18. Istvan ES, Dharia NV, Bopp SE, Gluzman I, Winzeler EA, Goldberg DE. 2011. Validation of isoleucine utilization targets in Plasmodium falciparum. Proc Natl Acad Sci U S A 108:1627–1632. http://dx.doi.org/10.1073/pnas.1011560108.

19. Hoepfner D, McNamara CW, Lim CS, Studer C, Riedl R, Aust T, McCormack SL, Plouffe DM, Meister S, Schuierer S, Plikat U, Hartmann N, Staedtler F, Cotesta S, Schmitt EK, Petersen F, Supek F, Glynne RJ, Tallarico JA, Porter JA, Fishman MC, Bodenreider C,

Diagana TT, Movva NR, Winzeler EA. 2012. Selective and specific inhibition of the plasmodium falciparum lysyl-tRNA synthetase by the fungal secondary metabolite cladosporin. Cell Host Microbe 11:654–663. http://dx.doi.org/10.1016/j.chom.2012.04.015.

20. Hoen R, Novoa EM, Lopez A, Camacho N, Cubells L, Vieira P, Santos M, Marin-Garcia P, Bautista JM, Cortes A, Ribas de Pouplana L, Royo M. 2013. Selective inhibition of an apicoplastic aminoacyl-tRNA synthetase from Plasmodium falciparum. Chembiochem 14:499–509. http://dx.doi.org/10.1002/cbic.201200620.

21. Keller TL, Zocco D, Sundrud MS, Hendrick M, Edenius M, Yum J, Kim YJ, Lee HK, Cortese JF, Wirth DF, Dignam JD, Rao A, Yeo CY, Mazitschek R, Whitman M. 2012. Halofuginone and other febrifugine derivatives inhibit prolyl-tRNA synthetase. Nat Chem Biol 8:311–317. http://dx.doi.org/10.1038/nchembio.790.

22. Alley MR, Baker SJ, Beutner KR, Plattner J. 2007. Recent progress on the topical therapy of onychomycosis. Expert Opin Investig Drugs 16:157–167. http://dx.doi.org/10.1517/13543784.16.2.157.

23. Hernandez VS, Ding C, Plattner JJ, Alley MRK, Rock F, Zhang S, Easom E, Li X, Zhou D. May 2012.Benzoxaborole derivatives for treating bacterial infections.European patent WO 2012033858.

24. Tumwebaze P, Conrad MD, Walakira A, LeClair N, Byaruhanga O, Nakazibwe C, Kozak B, Bloome J, Okiring J, Kakuru A, Bigira V, Kapisi J, Legac J, Gut J, Cooper RA, Kamya MR, Havlir DV, Dorsey G, Greenhouse B, Nsobya SL, Rosenthal PJ. 2015. Impact of antimalarial treatment and chemoprevention on the drug sensitivity of malaria parasites isolated from Ugandan children. Antimicrob Agents Chemother 59:3018–3030. http://dx.doi.org/10.1128/AAC.05141-14.

25. Shenai BR, Semenov AV, Rosenthal PJ. 2002. Stage-specific antimalarial activity of cysteine protease inhibitors. Biol Chem 383:843–847.

26. Guler JL, Freeman DL, Ahyong V, Patrapuvich R, White J, Gujjar R, Phillips MA, DeRisi J, Rathod PK. 2013. Asexual populations of the human malaria parasite, Plasmodium falciparum, use a two-step genomic strategy to acquire accurate, beneficial DNA amplifications. PLoS Pathog 9:e1003375. http://dx.doi.org/10.1371/journal.ppat.1003375.

27. Langmead B, Trapnell C, Pop M, Salzberg SL. 2009. Ultrafast and memory-efficient alignment of short DNA sequences to the human genome. Genome Biol 10:R25. http://dx.doi.org/10.1186/gb-2009-10-3-r25.

28. Kent WJ, Sugnet CW, Furey TS, Roskin KM, Pringle TH, Zahler AM, Haussler D. 2002. The human genome browser at UCSC. Genome Res 12:996–1006. http://dx.doi.org/10.1101/gr.229102.

29. Kabsch W. 1993. Automatic processing of rotation diffraction data from crystals of initially unknown symmetry and cell constants. J Appl Crystallogr 26:795. http://dx.doi.org/10.1107/S0021889893005588.

30. Otwinowski Z, Minor W. 1997. Processing of X-ray diffraction data collected in oscillation mode. Methods Enzymol 276:307–326. http://dx.doi.org/10.1016/S0076-6879(97)76066-X.

31. Collaborative Computational Project N. 1994. The CCP4 suite: programs for protein crystallography. Acta Crystallogr D Biol Crystallogr 50:760–763. http://dx.doi.org/10.1107/S0907444994003112.

32. McCoy AJ, Grosse-Kunstleve RW, Storoni LC, Read RJ. 2005. Likelihood-enhanced fast translation functions. Acta Crystallogr D Biol Crystallogr 61:458–464. http://dx.doi.org/10.1107/S0907444905001617.

33. Emsley P, Cowtan K. 2004. Coot: model-building tools for molecular graphics. Acta Crystallogr D Biol Crystallogr 60:2126–2132. http://dx.doi.org/10.1107/S0907444904019158.

34. Murshudov GN, Vagin AA, Dodson EJ. 1997. Refinement of macromolecular structures by the maximum-likelihood method. Acta Crystallogr D Biol Crystallogr 53:240–255. http://dx.doi.org/10.1107/S0907444996012255.

35. Aurrecoechea C, Brestelli J, Brunk BP, Dommer J, Fischer S, Gajria B, Gao X, Gingle A, Grant G, Harb OS, Heiges M, Innamorato F, Iodice J, Kissinger JC, Kraemer E, Li W, Miller JA, Nayak V, Pennington C, Pinney DF, Roos DS, Ross C, Stoeckert CJ, Jr, Treatman C, Wang H. 2009. PlasmoDB: a functional genomic database for malaria parasites. Nucleic Acids Res 37:D539–D543. http://dx.doi.org/10.1093/nar/gkn814.

36. Ashburner M, Ball CA, Blake JA, Botstein D, Butler H, Cherry JM, Davis AP, Dolinski K, Dwight SS, Eppig JT, Harris MA, Hill DP, Issel-Tarver L, Kasarskis A, Lewis S, Matese JC, Richardson JE, Ringwald M, Rubin GM, Sherlock G. 2000. Gene ontology: tool for the unification of biology. The Gene Ontology Consortium. Nat Genet 25:25–29.

37. Cusack S. 1997. Aminoacyl-tRNA synthetases. Curr Opin Struct Biol 7:881–889. http://dx.doi.org/10.1016/S0959-440X(97)80161-3.

38. Palencia A, Crepin T, Vu MT, Lincecum TL, Jr, Martinis SA, Cusack S. 2012. Structural dynamics of the aminoacylation and proofreading func-

tional cycle of bacterial leucyl-tRNA synthetase. Nat Struct Mol Biol **19:** 677–684. http://dx.doi.org/10.1038/nsmb.2317.

39. **Seiradake E, Mao W, Hernandez V, Baker SJ, Plattner JJ, Alley MR, Cusack S.** 2009. Crystal structures of the human and fungal cytosolic leucyl-tRNA synthetase editing domains: a structural basis for the rational design of antifungal benzoxaboroles. J Mol Biol **390:**196–207. http://dx .doi.org/10.1016/j.jmb.2009.04.073.

40. **Lincecum TL, Jr, Tukalo M, Yaremchuk A, Mursinna RS, Williams AM, Sproat BS, Van Den Eynde W, Link A, Van Calenbergh S, Grotli M, Martinis SA, Cusack S.** 2003. Structural and mechanistic basis of pre- and posttransfer editing by leucyl-tRNA synthetase. Mol Cell **11:**951–963. http://dx.doi.org/10.1016/S1097-2765(03)00098-4.

41. **Mursinna RS, Lincecum TL, Jr, Martinis SA.** 2001. A conserved threonine within Escherichia coli leucyl-tRNA synthetase prevents hydrolytic editing of leucyl-tRNALeu. Biochemistry **40:**5376–5381. http://dx.doi.org /10.1021/bi002915w.

42. **Ding D, Meng Q, Gao G, Zhao Y, Wang Q, Nare B, Jacobs R, Rock F, Alley MR, Plattner JJ, Chen G, Li D, Zhou H.** 2011. Design, synthesis, and structure-activity relationship of Trypanosoma brucei leucyl-tRNA synthetase inhibitors as antitrypanosomal agents. J Med Chem **54:**1276– 1287. http://dx.doi.org/10.1021/jm101225g.

43. **Obrig TG, Culp WJ, McKeehan WL, Hardesty B.** 1971. The mechanism by which cycloheximide and related glutarimide antibiotics inhibit peptide synthesis on reticulocyte ribosomes. J Biol Chem **246:**174–181.

44. **Schneider-Poetsch T, Ju J, Eyler DE, Dang Y, Bhat S, Merrick WC, Green R, Shen B, Liu JO.** 2010. Inhibition of eukaryotic translation elongation by cycloheximide and lactimidomycin. Nat Chem Biol **6:**209– 217. http://dx.doi.org/10.1038/nchembio.304.

45. **Jackson KE, Habib S, Frugier M, Hoen R, Khan S, Pham JS, Ribas de Pouplana L, Royo M, Santos MA, Sharma A, Ralph SA.** 2011. Protein translation in Plasmodium parasites. Trends Parasitol **27:**467–476. http: //dx.doi.org/10.1016/j.pt.2011.05.005.

46. **Khan S, Sharma A, Jamwal A, Sharma V, Pole AK, Thakur KK, Sharma A.** 2011. Uneven spread of cis- and trans-editing aminoacyl-tRNA synthetase domains within translational compartments of P. falciparum. Sci Rep **1:**188.

47. **Fidock DA, Rosenthal PJ, Croft SL, Brun R, Nwaka S.** 2004. Antimalarial drug discovery: efficacy models for compound screening. Nat Rev Drug Discov **3:**509–520. http://dx.doi.org/10.1038/nrd1416.

48. **Bowers GD, Tenero D, Patel P, Huynh P, Sigafoos J, O'Mara K, Young GC, Dumont E, Cunningham E, Kurtinecz M, Stump P, Conde JJ, Chism JP, Reese MJ, Yueh YL, Tomayko JF.** 2013. Disposition and metabolism of GSK2251052 in humans: a novel boron-containing antibiotic. Drug Metab Dispos **41:**1070–1081. http://dx.doi.org/10.1124/dmd .112.050153.

49. **Ciaravino V, Plattner J, Chanda S.** 2013. An assessment of the genetic toxicology of novel boron-containing therapeutic agents. Environ Mol Mutagen **54:**338–346. http://dx.doi.org/10.1002/em.21779.

50. **Zhang YK, Plattner JJ, Freund YR, Easom EE, Zhou Y, Gut J, Rosenthal PJ, Waterson D, Gamo FJ, Angulo-Barturen I, Ge M, Li Z, Li L, Jian Y, Cui H, Wang H, Yang J.** 2011. Synthesis and structure-activity relationships of novel benzoxaboroles as a new class of antimalarial agents. Bioorg Med Chem Lett **21:**644–651. http://dx.doi.org /10.1016/j.bmcl.2010.12.034.